

An in situ benthic chamber system for improved temporal and spatial resolution measurement of sediment oxygen demand

Kara J. Gadeken    * Grant Lockridge,  Kelly M. Dorgan   

¹Dauphin Island Sea Lab, Dauphin Island, Alabama, USA

²University of South Alabama, Mobile, Alabama, USA

Abstract

In shallow coastal systems, sediments are exposed to dramatic and complex variability in environmental conditions that influences sediment processes on short timescales. Sediment oxygen demand (SOD), or consumption of oxygen by sediment-dwelling organisms and chemical reactions within sediments, is one such process and an important metric of aquatic ecosystem functioning and health. The most common instruments used to measure SOD in situ are batch-style benthic chambers, which generally require long measurement periods to resolve fluxes and thus do not capture the high temporal variability in SOD that can be driven by dynamic coastal processes. These techniques also preclude linking changes in SOD through time to specific features of the sediment, for example, shifts in sediment faunal activities which can vary on short time scales and can also be affected by ambient oxygen concentrations. Here we present an in situ semi-flow through instrument to repeatedly measure SOD in discrete areas of sediment. The system isolates patches of sediment in replicate benthic chambers, and measures and records oxygen decrease for a short time before refreshing the overlying water in the chamber with water from the external environment. This results in a sawtooth pattern in which each tooth is an incubation, providing an automated method to produce direct measurements of in situ SOD that can be directly linked to an area of sediment and related to rapid shifts in environmental conditions.

Sediment oxygen demand (SOD) is a crucial metric for assessing the health and function of marine ecosystems (Jørgensen et al. 2022; Middelburg and Levin 2009). Coastal sediments are the site of intensive remineralization of organic matter, making them a major sink of dissolved oxygen (DO) via aerobic respiration and reduced metabolite reoxidation, particularly in sediments with minimal benthic primary production (Burdige 2006). A given area of sediment in a shallow coastal setting may also be exposed to large-ranging and rapidly-varying environmental conditions driven by changes in light exposure, temperature, salinity, flow regimes, and deposition (Wenner et al. 2004). This results in coastal sediments being patchy on small spatial scales.

The dynamism of coastal systems drives similarly dynamic benthic fluxes, yet very few studies have captured this variability on relevant temporal and spatial scales. This lack of

knowledge can in part be explained by the methodological challenges of measuring fluxes in situ. A long-used method of measuring chemical fluxes in the field is the “batch-style” (completely enclosed) benthic metabolism chamber, commonly deployed once or a few times in a day (Tengberg et al. 1995). Because it must be manually deployed for each measurement, the batch metabolism chamber generates a very low temporal resolution of data and usually restricts measurements to daylight hours. However, it does allow measurements to be associated with discrete areas of sediment and so captures spatial variability when used with sufficient replication. To overcome the temporal limitations, some researchers have also modified the typical chamber methods by deploying chambers for longer and periodically opening the chamber to allow flushing of the enclosed water, which effectively starts a new incubation (Wenzhöfer and Glud 2004). Researchers have also developed a flume-style chamber that better replicates horizontal flow and allows for high-frequency measurement of oxygen consumption, albeit over a relatively larger area and with a greater incubated volume of water (Camillini et al. 2021). Researchers have noted that measurements acquired from benthic chambers tend to underestimate SOD because the chamber structure restricts advective flow, particularly in permeable sediments that experience flow-induced

*Correspondence: kgadeken@disl.org

Author Contribution Statement: KJG designed, constructed, and tested the instrument with critical guidance and assistance from GL and mentorship from KMD. KJG wrote the manuscript with advice and editing input from KMD.

Additional Supporting Information may be found in the online version of this article.

porewater flushing (Berg *et al.* 2013; Attard *et al.* 2015). However, chambers are relatively simple to construct and deploy and can be tailored to specific environments or applications, features which have made them the primary tool for measuring benthic fluxes *in situ*.

More recently, the eddy covariance technique, used for decades to measure fluxes in the atmospheric sciences, has been adapted for use in various aquatic systems to collect *in situ* measurements of benthic fluxes (Berg *et al.* 2003, 2009; Attard *et al.* 2015; Juska and Berg 2022). With this technique, SOD for a given area of the seafloor can be calculated from point measurements of dissolved oxygen and the velocity field taken above the benthos. This allows for more continuous measurement of fluxes over time than is typical with benthic chambers and the method can capture diel variability (Berg *et al.* 2022). Another distinct advantage is the open design; unlike benthic chambers, eddy covariance does not require the enclosure of a portion of the benthos and thus does not obstruct natural flow conditions. However, this means that natural variability in flow rates and directions change the size and shape of the area contributing to the flux, so eddy covariance is most appropriately viewed as a spatially-averaged flux measurement technique for a relatively large seafloor area (usually between 10 and 100 m²) (Berg *et al.* 2007). Though such ecosystem-scale measurements are certainly valuable, many benthic habitats are characterized by high patchiness on small spatial scales (e.g., coral reefs, microbial mats, macrophytes, unevenly distributed deposits of organic matter, etc.) and eddy covariance cannot distinguish the relative contributions of the patchy elements that compose the system. In sediments, for example, macrofaunal behaviors typically influence SOD in a highly localized volume around their tube or burrow structure (Aller 1978; Zorn *et al.* 2006; Volkenborn *et al.* 2010), and eddy covariance lacks the spatial resolution to determine how the presence or absence of macrofauna may affect SOD.

The existing methods to measure SOD *in situ* are optimized to either capture temporal or spatial variability but are currently insufficient to describe the relationship between the two. We have built a chamber system to better capture temporal resolution than typical single-deployment batch chambers, while also sampling small-scale spatial variation. Its potential applications are broad; for example, if deployed with some chambers transparent and others shaded, the system could inform on light-driven variations in net metabolism, and due to the short incubation periods may mitigate the common issue of DO supersaturation and bubble production within the chambers. By performing a parallel incubation designating some chambers to incubate sediment while others incubate water alone, the system could measure shifts in the relative contributions of the water column and benthic respiration in eutrophic settings with highly variable environmental conditions. There are compelling possibilities for doing manipulative experiments in the field, for example, by enriching

sediments with organic matter or populating with select macrofauna, and then deploying the chamber system to collect high-frequency flux data and gauge benthic response *in situ*. Depending on the application and experimental objectives, the system could also be fitted with additional sensors and water sampling ports to provide coupled measurements of dissolved inorganic carbon, pH, or other relevant parameters.

This setup and methodology will allow for an improved description of the complex relationship between environmental variability, spatial heterogeneity, and benthic fluxes in shallow systems. The system was constructed for use in a field study to measure SOD throughout a diel cycle and evaluate the effect of the presence of sediment macrofauna on dynamic changes in SOD. The full results of this study will be presented in a forthcoming research paper, and here we present only the data necessary to demonstrate the functioning of the chamber system.

Materials and procedures

The system was designed to take repeated measurements of SOD in replicate benthic chambers and is composed of a central housing for power and electronics and five chambers that are tethered to the central housing (Fig. 1A). The central housing for power and electronics (Fig. 1B) controls submersible pumps attached to the chambers (Fig. 1C) and is programmed to periodically turn on each chamber pump (flush pumps) for a short time to flush the overlying water with water of ambient dissolved oxygen concentration from the environment. DO is measured in each chamber by an Onset HOBO DO logger, and SOD can be found from the slope of the decrease in DO in each measurement period. Over an entire deployment, this results in the DO within the chambers following a saw-tooth pattern, with the slope of each tooth being a SOD incubation (Fig. 2). To mix the overlying water and prevent stagnation in between water exchanges, a small, enclosed impeller was outfitted with two neodymium magnets (0.375" W × 0.125" H) arranged with opposite polarity to magnetically couple with a stir bar (5/16" OD × 1" L) through the chamber lid (Supporting Information S1). When water is pumped through the impeller enclosure, the impeller spins, mixing the water in the chamber. A single pump (mixing pump) plumbed in series with five benthic chambers provided all mixing actions simultaneously.

The central housing is constructed from 6-in. diameter (15.24 cm) schedule 40 clear PVC tubing, capped on each end with a PVC-glued plastic flange, rubber gasket, and plastic endpiece which was secured with six 3/4 × 10 × 3.5 long bolts and nuts (Fig. 1B; Table 1). One endpiece has a SeaCon AWQ 4/24 6-port bulkhead mounted to connect the submersible pumps outside the housing to the electronics and power source inside the housing. The housing was seal-tested by deploying it at 20 m for ~48 h and we found no evidence of

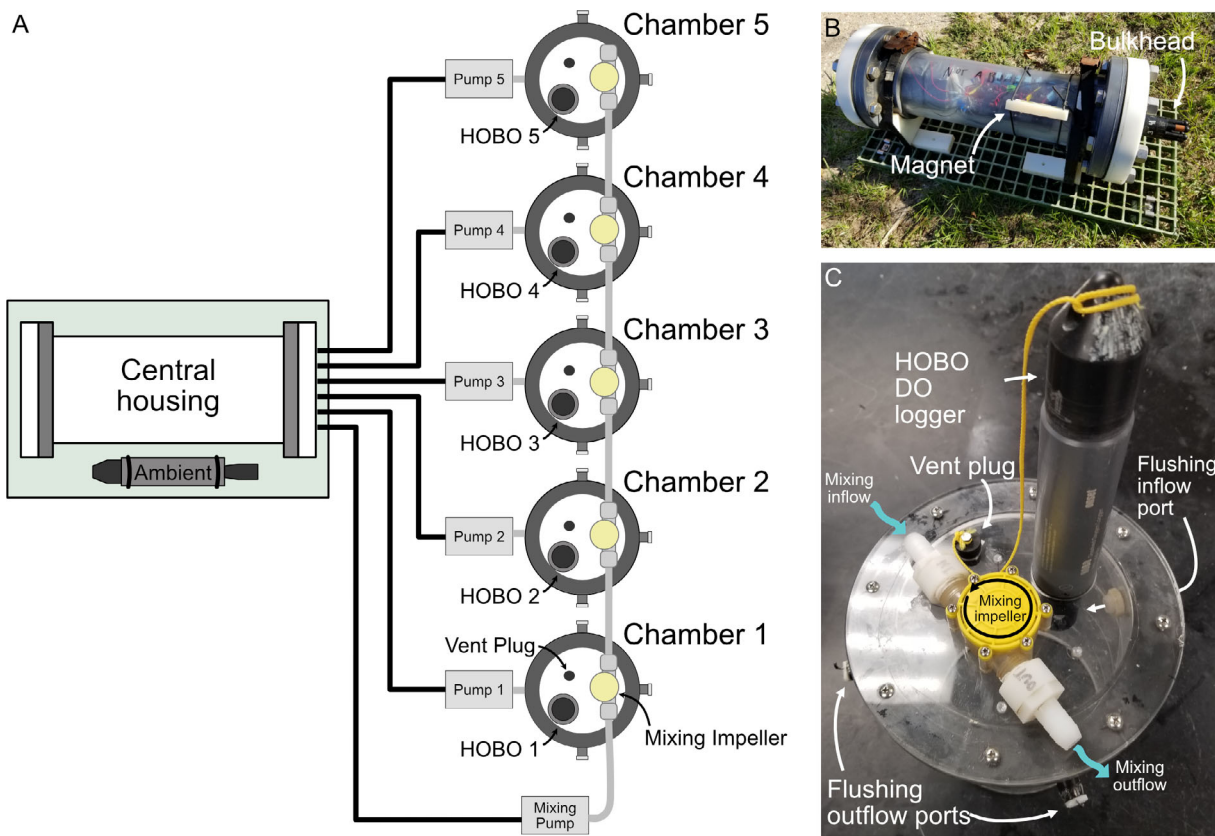


Fig. 1. (A) Central housing and chamber setup schematic diagram and photos of (B) the central housing and (C) one of the benthic chambers. The central housing contains the batteries and electronics and the pumps are controlled via connections through a wet-mate bulkhead. The HOBO taking the ambient DO measurement is secured to the platform with the chamber housing. The housing is mounted to a rigid fiberglass platform for deployments. Once the housing and chambers are deployed and the pumps connected, the external magnet is moved into alignment with the internal magnetic switch to turn the system on. During a measurement period, the flushing pumps (pumps 1–5) sequentially turn on to flush the overlying water in the chambers, and then the mixing pump is intermittently turned on to agitate the overlying water of all the chambers to prevent stagnation.

leaks after recovery. A 13.5 V battery pack in the central housing powers the electronics and the pumps (Supporting Information S2). The battery pack consists of three units connected in parallel, with each unit having nine 1.5 V D cell batteries connected in series. A spot welder was used to make the electrical connections between batteries and battery units and the entire battery pack was secured together with duct tape. Six SeaBird 5T/5P submersible 12 V pumps were used for this build with the appropriate plug configuration to fit the bulkhead. An Arduino Uno microcontroller was used to control the pump cycling via 12 V relays and recorded the start time of each measurement period with an Adafruit Data Logging Shield. Power to the device is cycled with a magnetic switch situated close to the housing wall so that the system can be turned on after the housing is sealed. When powered on, the Arduino immediately begins executing the programmed code on a loop, with each loop representing a single measurement period. At the start of a loop, the Arduino records the date and time and then sequentially turns each chamber flush pump

on for 20 s to flush the overlying water in the chamber with water of ambient DO concentration. The code then executes 20 repetitions of turning the mixing pump on for 15 s and off for 45 s to mix the overlying water in the chambers and prevent stagnation. The loop then concludes and starts again. The duration of the measurement period (in min) is therefore determined by the number of times that the Arduino is programmed to turn the mixing pump on and off. The annotated Arduino code can be found in the Supporting Information S3.

Five replicate benthic chambers were constructed. To construct a benthic chamber, an acrylic flange was glued to one end of a 6-in. ID clear acrylic tube, and a top cap was secured in place with stainless steel screws (6-32) with a gasket between the flange and cap (Fig. 1C; Supporting Information S1). The top cap had a CNC-milled hole for attaching the HOBO dissolved oxygen logger and a smaller vent hole to allow for the escape of any air bubbles and to vent water displaced during chamber deployment. Once

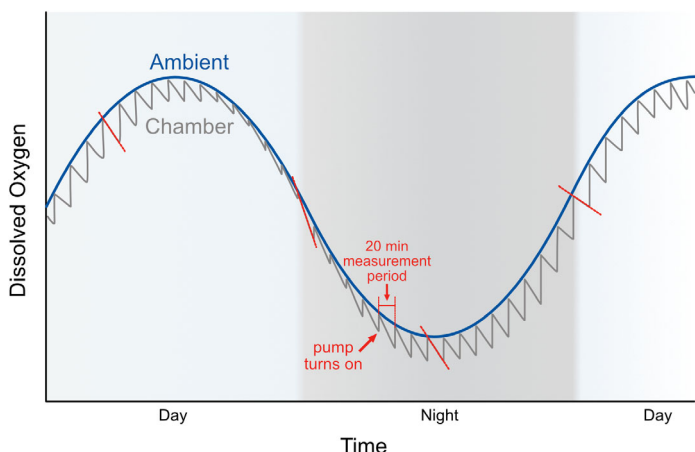


Fig. 2. Conceptual diagram of a diel oxygen cycle from the ambient DO measurement (blue line) and the “sawtooth” pattern from the DO in one of the benthic chambers (gray line). The gray-shaded section of the plot indicates nighttime hours. Each measurement period is ~ 20 min. When the chamber pump is turned on, the overlying water is flushed with water of ambient DO concentration to start another measurement period. Slopes of the teeth can be compared at different times in the deployment to gauge change in SOD (red dashed line segments).

deployed, a rubber stopper is placed in the vent hole opening to prevent water exchange. Screw holes were drilled in the top cap to mount the mixing impeller housing (Supporting Information S1), and the magnetically coupled stir bar was suspended from the underside of the top cap beneath the impeller housing with a fishing swivel to allow it to rotate freely.

The chamber has one inflow and three outflow ports (½ in. diameter) for flushing the overlying water. The outflow ports are fitted with one-way valves constructed from negatively buoyant plastic caps each threaded on a wire hook. When the chamber is flushed the caps swing upwards and allow water to easily exit, and during the measurement period, the caps cover the port openings to prevent backflow. The sediment surface area enclosed by a chamber is 0.017 m², and when pushed into the sediment allowing for 5 cm of water height within the chamber, encloses 0.9 L of overlying water.

Assessment

Design concept and development

The setup was constructed through an iterative process of testing and troubleshooting with the objective of potentially using the system in a variety of environments and at a range of water depths, which informed the rugged design of the central housing, the use of high depth-rated submersible pumps and the decision to mix chambers with pump-driven impellers. This resulted in a simplified design that can be expected to function similarly in dynamic, shallow subtidal waters and the deeper waters on the continental shelf.

System testing

We performed operational tests on the chambers in the lab and confirmed that the chamber overlying water was sufficiently enclosed during incubations to obtain SOD measurements (Supporting Information S4, S5). In laboratory benthic metabolism chambers the overlying water is typically mixed continuously, however, with in situ systems maintaining effective mixing can be a challenge. A variety of mixing strategies have been used with in situ chambers, from battery-powered mechanisms mounted to the top of each chamber to paddle wheels that transfer ambient flow energy to the chamber interior (Tengberg et al. 1995). Because of the long deployment time of our in situ chambers, individual battery-powered stirring mechanisms were impractical, and paddle wheels would introduce problematic variability because of the inconsistency of ambient flow rates over time. The mixing apparatus for our system allows for the simultaneous mixing of all the chambers using only one pump, and we set the system to mix the chambers intermittently instead of continuously to conserve battery power for the long deployment. To estimate the effect of intermittent mixing on SOD, we set up two sample chambers in a lab flume with the mixing apparatuses hooked up in series and ran the system for several measurement periods while intermittently and continuously mixing (Fig. 3A). There was no significant difference between SOD when the chambers were being intermittently vs. continuously mixed for either chamber (Fig. 3B; one-way ANOVA, $p > 0.05$), so for deployments, the system was set to mix intermittently. Flow velocity and direction affect the thickness of the diffusive boundary layer at the sediment–water interface, and in permeable sediments can result in pressure gradients forming within the chamber that drives artificial porewater advection and sediment flux (Glud et al. 1996; Tengberg et al. 2004; Arega and Lee 2005). Our test site was shallow and frequently subject to strong wave action driving oscillatory flow which would result in constantly shifting benthic boundary layer dynamics and pressure gradients. Given the typical flow dynamics of the site, intermittent mixing was deemed sufficient for our application, however, in settings with more directional flow more consistent mixing would be preferred.

The system was field tested in Gulf Shores, Alabama, U.S.A., at a shallow (< 1 m), sandy site in Bon Secour Bay, a partially enclosed embayment in southeast Mobile Bay (30.239478°, -87.894094°). Bon Secour experiences relatively slow exchange and long water residence times compared to the flushing dynamics of the rest of Mobile Bay (Webb and Marr 2016; Du et al. 2018). A previous sampling at this site had revealed a patchily distributed community of infauna co-occurring with clusters of the large tube-building Onuphid polychaete *Diopatra cuprea*, providing an optimal setting to capture spatial variability in macrofaunal effects. The sediment type was clean granular sand and the site regularly experienced intense wave action generated from winds blowing

Table 1. Materials and components list.

	Source	Notes
Central housing components		
6" Sched 40 clear PVC pipe	US plastic	Item#: 34113
6" Sched 80 PVC socket companion flange (× 2)	US plastic	Item#: 28165
6" neoprene flange gasket (× 2)	US plastic	Item#: 28170
Endcaps (× 2)	US plastic	Item#: 45426 (custom-milled)
18-8 SS hex head screws	McMaster-Carr	Item#: 92186A851
316 SS hex nuts	McMaster-Carr	Item#: 97619A660
316 SS washers	McMaster-Carr	Item#: 90107A121
Arduino Uno Rev3 SMD	Arduino	Code: A000073
SD data logging shield for Arduino	Adafruit	Product ID: 1141
SD card	Amazon	Sandisk 32GB
12 V FeatherWing power relay	Adafruit	Product ID: 3191
Power and ground distribution blocks	Amazon	1/4" Stud Junction Bus bar Kits
Magnetic switch	McMaster-Carr	Item#: 8073A28
Terminal connectors	Amazon	Strip blocks with spring clips
Bulkhead	SeaCon	AWQ 4/24 6-port
Submersible pumps	Seabird scientific	SBE5P, PL, MCBH, STD VOLT, 3000 RPM, SLOW ST
Pump connector (× 6)	Tti	TTI part number: MC-S061-0060
Bulkhead connector (× 6)	Tti	TTI part number: AWQ-S011
Splice kits	Zoro	Zoro#: G2179484
Chamber components		
6" OD acrylic tubing (chamber body)	US plastic	Item#: 44550
12 mm cast acrylic sheet (chamber flange)	US plastic	Item#: 44381 (custom-milled)
5.6 mm extruded acrylic sheet (chamber top)	US plastic	Item#: 44350 (custom-milled)
1/16" gasket material	McMaster-Carr	Item#: 8635K162
6-32 thread 316 SS truss head screws, 1" long	McMaster-Carr	Item#: 94792A717
6-32 thread 316 SS serrated flange locknuts	McMaster-Carr	Item#: 91343A101
Vent port plug	McMaster-Carr	Item#: 9545K115
Mixing impeller	Amazon	Water turbine generator was retrofitted by removing the internal electronics and installing magnets in the impeller
Magnets	McMaster-Carr	Item#: 5862K143
Magnetic stir bar	McMaster-Carr	Item#: 5678K143
Mixing impeller hose barb fittings	McMaster-Carr	Item#: 5372K182
Outflow and inflow port fittings	McMaster-Carr	Item#: 5218K704
Outflow port locknuts	McMaster-Carr	Item#: 7877 N103
HOBO DO logger	Onset	Part#: U26-001
1/2" ID rubber tubing	McMaster-Carr	Item#: 5233K68
Outflow caps	McMaster-Carr	Item#: 8546K12 (custom-made from nylon rod)

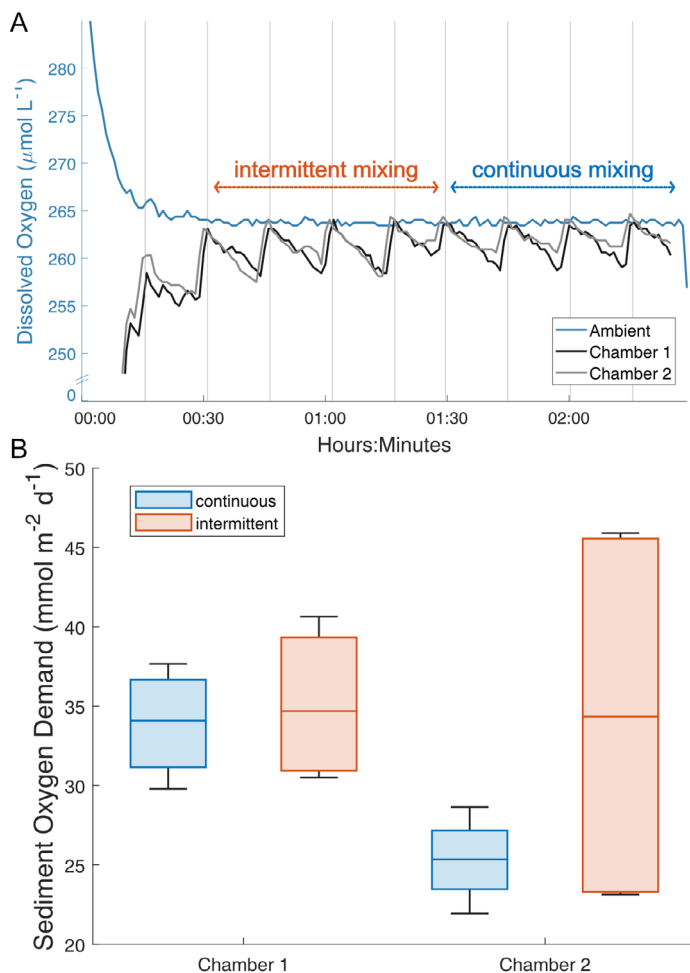


Fig. 3. Results of mixing test in laboratory flume for two benthic chambers with sediment. The system was programmed to mix in cycles of 20 s on : 40 s off for several measurement periods, and then the system was switched to mix continuously for several measurement periods (A). Vertical gray lines mark the beginning of each measurement period. There was no significant difference between SOD measurements when continuously mixing vs. intermittently mixing for either chamber (B) ($p > 0.05$).

across the bay, which offered an opportunity to test the limits of the system in an energetic flow regime and in permeable sediments.

All HOBO loggers were two-point calibrated the day before deployment. The central housing was secured to a fiberglass grid mesh platform (Fig. 1B). An additional HOBO DO logger was mounted to the housing platform to measure the ambient DO concentration. The benthic chambers were deployed in a line at the bulkhead end of the housing. Each chamber was pushed down 15 cm into the sediment which left a 5 cm vertical height of overlying water enclosed in the chamber. The flush pumps were attached to the inflow ports on each of the chambers. The mixing pump was attached to a PVC pole embedded into the sediment so that the pump intake was suspended in the water column. Flexible PVC tubing (½ in. ID) was plumbed from the mixing pump outflow and

connected in series between the mixing impellers on the tops of all the chambers. Before deployment, the transparent surfaces of all the chambers were covered in duct tape to prevent photosynthesis inside the chambers during daylight hours.

The system was deployed from shore and recovered ~ 24 h later. The salinity recorded at the time of deployment was 18. At recovery, the chambers were extracted from the benthos with the enclosed sediment intact. The contents were then sieved in the field through a 1 mm mesh sieve and preserved in 70% EtOH with Rose Bengal to stain faunal tissue. DO data were offloaded from each of the 5 chamber HOBO loggers and the ambient DO HOBO logger, plotted to observe the DO pattern throughout the diel cycle and analyzed for SOD.

To properly test the system, we first had to confirm that (1) the ambient DO followed a diel cycle. The system was gauged to have operated successfully if, (2) the DO in the chambers exhibited the sawtooth pattern in relation to the ambient DO, (3) the chamber DO at each sawtooth peak matched the ambient DO at that time (indicating sufficient chamber flushing), and (4) SOD measurements could be collected throughout the diel cycle.

Diel cycle

The ambient DO measured by the HOBO DO logger attached to the central housing platform roughly followed a diel cycle, with the maximum DO concentration of $398.4 \mu\text{mol L}^{-1}$ at 17:25 h and the minimum DO concentration of $106.9 \mu\text{mol L}^{-1}$ at 01:34 h (Fig. 4). In a diel cycle minimum DO typically occurs near dawn (~ 06:30 h here), however there is a noticeable dip and rise in DO concentrations between 23:00 and 02:00 h during the deployment. Low tide occurred at approximately 22:00 h, and we suspect that the flooding tide moved a parcel of deoxygenated bottom water from deeper in Mobile Bay to our site and caused the period of lower DO observed in the data.

Sawtooth pattern

Chambers 2–5 show distinct sawtooth patterns with clear variations in the slope steepness between the different chambers, however, chamber 1 appears to have malfunctioned for much of the deployment (Fig. 4). We observed that the flush pump associated with chamber 1 was malfunctioning when the system was recovered. Because of a faulty electrical connection, the pump would sometimes turn on when it was programmed to but often would not. We believe that this was occurring throughout the deployment, which is why much of the data for that chamber does not follow the consistent sawtooth pattern seen in the other chambers. Interestingly, it appears that for a few hours at the end of the deployment the chamber was functioning properly, as evidenced by the sawtooth from ~ 06:00 to 09:00 h (Fig. 4A). However, because most of the chamber 1 data for the deployment was very obviously not valuable, and we were interested in evaluating how the system performed throughout the diel cycle, we decided to exclude chamber 1 from further analysis.

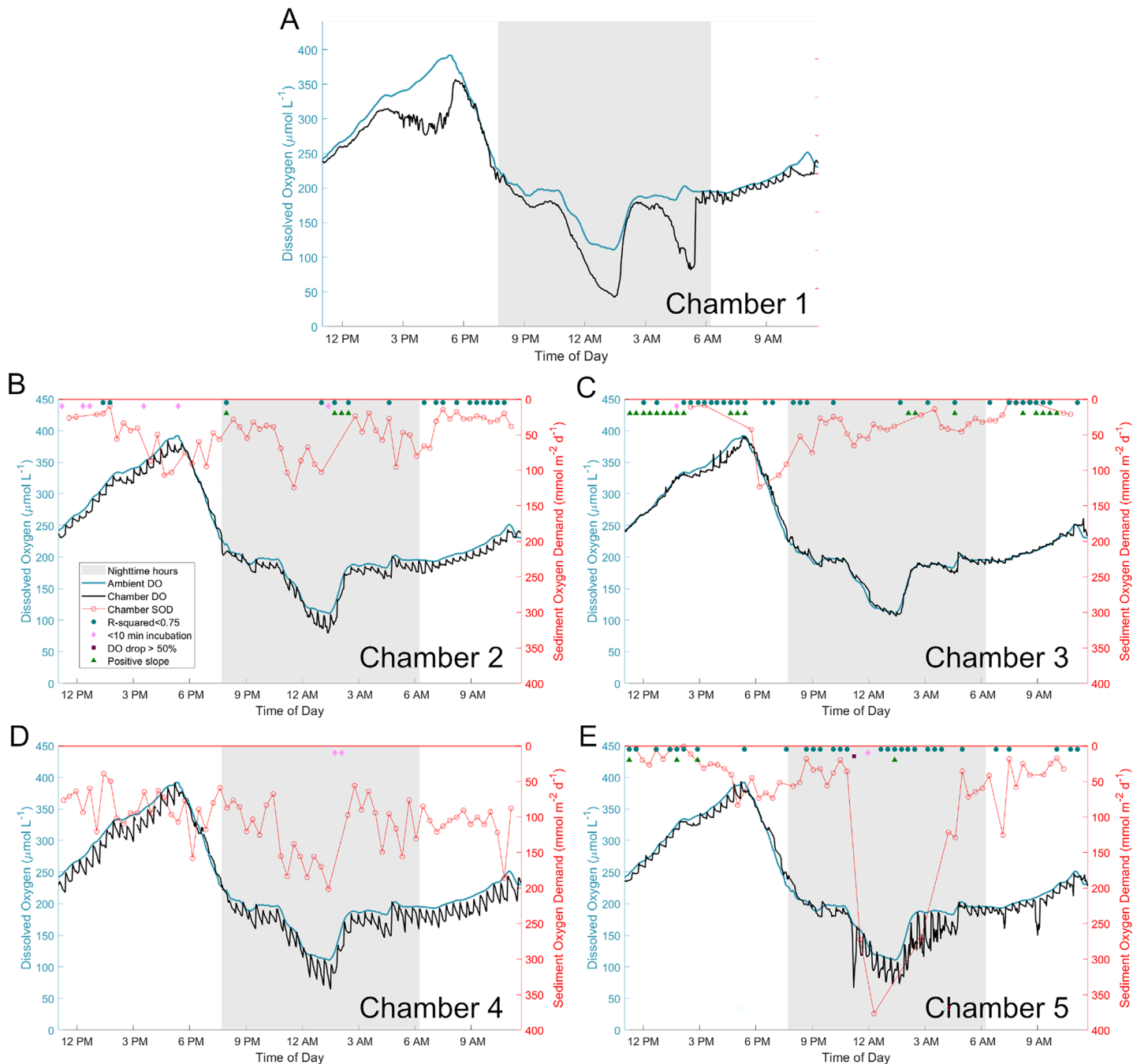


Fig. 4. Ambient DO (blue lines, data smoothed with 12-point moving average), chamber DO (black lines), and calculated SOD values (red points) from test deployment. Gray-shaded areas are nighttime hours delineated by times of sunset and sunrise. The chamber DO exhibits the desired “sawtooth” pattern in chambers 2–5. Chamber 1 appears to have malfunctioned for much of the deployment so was excluded from the SOD analysis. SOD was calculated from the slopes of each of the measurement periods for chambers 2–5; measurements from slopes with regression fits (R^2) below 0.75 (blue circles), slopes that were calculated from incubations shorter than 10 min (pink diamonds), and measurements that were taken during an incubation in which the DO in the chamber decreased by more than 50% of the starting DO (red squares) or had a positive slope (green triangles) were excluded. Measurements with both a SOD value and a blue circle are those that were flagged due to their low R^2 but included based on visual inspection.

Chamber flushing

To determine whether the chambers were being adequately flushed, the difference between the ambient DO and the

chamber DO concentrations directly after the flush step of each measurement period (i.e., at the sawtooth “peaks”) were plotted against the ambient DO concentrations for chambers

2–5 (Fig. 5). Values close to zero indicate that the chamber DO was similar to the ambient DO after being flushed. The maximum deviation of the flushed chamber DO from the ambient was $-16.9 \mu\text{mol L}^{-1}$ (in chamber 4), and for every chamber at least 85% of chamber DO values after flushing were within $\pm 7.8 \mu\text{mol L}^{-1}$ of their corresponding ambient DO. The accuracy of the DO measurements taken by the HOBO loggers is $\pm 6.25 \mu\text{mol L}^{-1}$ up to $250 \mu\text{mol L}^{-1}$, and $\pm 15.6 \mu\text{mol L}^{-1}$ from 250 to $625 \mu\text{mol L}^{-1}$ (Johengen *et al.* 2016). Our measurements are relatively well constrained within the accuracy ranges of the sensors, indicating that the chamber DO measurements directly after flushing were similar to the ambient DO measurements and that the chambers were being sufficiently flushed throughout the deployment.

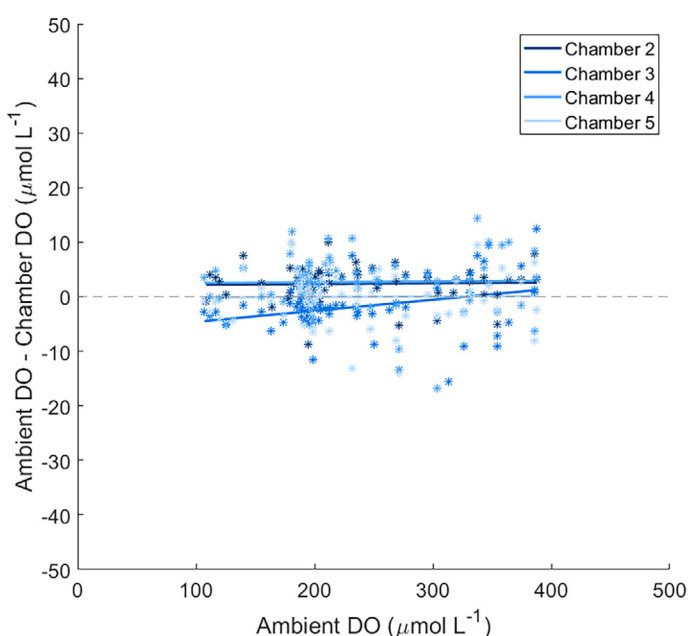


Fig. 5. Difference between the ambient DO and the simultaneous chamber DO directly after the flush step of each measurement period, plotted against the ambient DO at that time for chambers 2–5. The dotted line at $y = 0$ indicates the chamber DO exactly matches the simultaneous ambient DO.

SOD measurements

SOD was calculated from the linear slopes of the chamber “teeth” for all measurement periods in the deployment (Fig. 4). Though many of our slopes were highly linear we also observed a variety of DO patterns within the incubations, ranging from irregular fluctuations to DO leveling off or drifting up near the end of the measurement period. In cases where slopes did not appear linear for the entire incubation duration, slopes were calculated from a subset of the incubation data gauged to be linear. We then removed low-quality or questionable SOD measurements from the data set based on certain criteria; we excluded measurements from slopes with regression fits (R^2) below 0.75, slopes calculated from incubations shorter than 10 min (or less than half of the measurement period), and measurements taken during incubations in which DO in the chamber decreased by more than 50% of the starting DO or had a positive slope (Fig. 4).

Excluding measurements based on R^2 value could severely bias the data because regressions with shallower slopes tend to have lower R^2 values than steeper-sloped regressions, given the same variability. This means that incubations with very low SOD (“flat” DO trends through time) would be disproportionately discarded even though they may reflect real patterns in the data. To account for this, all incubations that were flagged as having R^2 values lower than the 0.75 thresholds were visually inspected, and those that were highly linear but with a flat trend through time were added back into the dataset, while those with irregular trends were discarded.

Discussion

SOD is a challenging parameter to measure, particularly in the field. This chamber setup demonstrates a novel methodology that can resolve fluxes for constrained areas of sediment and at a high frequency, in conditions closely resembling in situ. While our application of the system was focused on the diel oxygen cycle, the methodology could be applied in diverse ways to answer a broad range of questions concerning the relationship between spatial and temporal variability in sediment processes.

Filtering yielded a data set of high-quality linear slopes (Table 2). The SOD measurements varied widely both between

Table 2. Chamber SOD measurements. Chamber 1 was excluded due to malfunction. Number of measurements refers to the total number of high-quality SOD incubations performed by the system for each chamber throughout the deployment. The mean and standard deviation were taken of this set of measurements, representing the average SOD expected from each chamber and the variation from this average that may be expected throughout the diel cycle.

Chamber #	Number of measurements	Mean SOD \pm std dev ($\text{mmol m}^{-2} \text{d}^{-1}$)	Faunal total wet biomass (g)
2	57	51.4 ± 28.6	0.03
3	36	39.0 ± 27.0	0.08
4	65	104.9 ± 36.0	0.53
5	47	60.0 ± 72.6	0.45

chambers and between measurements by a single chamber, though these values are not unusual when compared to SOD measurements more broadly in coastal regions (Jørgensen et al. 2022) and more specifically from other studies conducted in permeable sediments in the Northern Gulf of Mexico. Nighttime benthic chamber measurements from a shallow (1–1.5 m) sandy site in Apalachicola Bay, FL, yielded SOD values of $98 \pm 21 \text{ mmol m}^{-2} \text{ d}^{-1}$ (Berg and Huettel 2008). Berg et al. (2013) reported nighttime SOD rates ranging from 50 to $120 \text{ mmol m}^{-2} \text{ d}^{-1}$ from benthic chambers deployed in permeable river sediments at a similar latitude to our test site, and the majority of SOD values collected from our setup fall in that range (Berg et al. 2013). It is worth noting that both these studies also simultaneously deployed eddy covariance systems, and in both cases, the nighttime SOD values from the eddy covariance method were markedly higher than the respective chamber incubation values ($368 \pm 21 \text{ mmol m}^{-2} \text{ d}^{-1}$ in Berg and Huettel 2008 and $359.8 \pm 24 \text{ mmol m}^{-2} \text{ d}^{-1}$ in Berg et al. 2013). Previous studies have shown that benthic chamber and eddy correlation measurements tend to be similar in cohesive sediments and sediments lacking large fauna. But particularly in permeable sands under dynamic flow conditions, chambers tend to yield lower fluxes because they restrict porewater advection-induced oxygen uptake (Attard et al. 2015).

In this system, it is necessary to enclose some portion of the sediment to associate measurements directly with particular areas of sediment and capture both spatial and temporal variability. It was also necessary for our application to shade the chambers to isolate the effect of changing oxygen concentrations on SOD without photosynthesis convoluting the measurements. However, shading and enclosure can affect SOD, and there are indications of such an effect in our data. In the evening portion of the deployment (Fig. 4, ~17:00–21:00 h), the DO inside the chambers appeared to be at a similar or even greater concentration than the ambient DO which was rapidly declining. During this period the chamber and ambient DO values match well directly after the chambers had been flushed and the DO measurements diverge as the incubations proceed, indicating that DO in the ambient environment was declining faster than in the incubated chambers. This is likely due to photosynthesis-coupled respiration occurring at high rates in the ambient environment outside the chambers that would not have been occurring in the shaded chamber interiors.

There were also several instances of DO slopes flattening out or drifting upwards near the end of incubations, or even for slopes to be slightly positive (Fig. 4). This may be a result of the permeability of these sediments that pressure gradients caused by flow allowing oxygenated water to invade the chambers, or it may be a limitation of the intermittent mixing scheme that oxygenated water may be mixed less evenly and therefore result in measurement irregularities. However, nonlinear oxygen decreases during chamber incubations are not uncommon,

particularly when bottom water oxygen concentrations are high (Kononets et al. 2021). In these cases, it can be difficult to discern which portion of the incubation represents the true flux rate, and this was the primary reason for filtering the data by linearity criteria and visually inspecting each slope for signs of drift. Even with these limitations and in a challenging environment, the semi-flow through chamber system was able to produce many highly linear replicate slopes and would only be expected to show improved performance in consolidated sediments or lower-flow conditions.

Filtering the data based on the stated quality criteria resulted in different numbers of useable measurement periods depending on the chamber, with a greater number of high-quality measurements generally produced in chambers with higher average SOD (Table 2). Chamber 5 is the exception; SOD increased dramatically in the nightly low DO period and DO in many of its incubations during that period followed a highly irregular pattern (and therefore excluded them from analysis) (Fig. 4E). There was also considerable variability between chambers and even between successive SOD measurements within a given chamber. Data from eddy covariance studies have indicated that SOD can vary widely on short timescales (on the order of minutes), a phenomenon also demonstrated in our measurements (Berg and Huettel 2008; Berg et al. 2013). Furthermore, in our setup the average SOD varied substantially between chambers (Fig. 4), suggesting variation on small spatial scales. We suspect that faunal activity may account both for the period of much greater SOD in Chamber 5 and for the irregular DO patterns. Further analysis of the changes in SOD throughout the diel cycle and their association with the faunal community will be presented in the forthcoming research paper.

Comments and recommendations

System construction

Our objective in building this system was to demonstrate the utility and practicability of the semi-flow through chamber concept, and we would advise those wishing to build a similar system to tailor it for their specific application. Several components in our setup were used because they were easy to access or already in our possession, however, depending on the application a more economical version of some components would do as well or better. For example, the flushing and mixing pumps used in our system are depth rated to 600 m, however, if the system will be used only in very shallow water we would advise using simple aquarium pumps and modifying the power connector with a wet-mate plug into the bulkhead. The system could likewise be scaled up or down depending on power requirements and logistical restrictions of deployment. Other aspects of the setup, such as the construction of the chamber outflow ports and the intermittent mixing scheme, provided the most workable solution during

development but could be further optimized in a new version, and we would encourage those intending to build their own system to experiment with alternatives.

System settings and deployment considerations

The Arduino code controlling the execution of the system has three major features that may be changed to adjust operation: the measurement period length, the flush duration, and the mixing settings.

The measurement period length is set by changing the number of iterations that the Mixing Pump is turned on or off and will control the duration of each “sawtooth.” Selecting a measurement period length requires striking the correct balance between collecting sufficient data for slope calculation and avoiding an excessive drop in DO. Because SOD is generally positively correlated with DO concentration (Burdige 2006), long incubations risk the chamber DO decreasing to the point of changing the SOD slope, resulting in a nonlinear pattern. However, short incubations may not provide enough time for a consistent pattern to appear. In addition, the measurement period selected must take into consideration how SOD may change throughout the diel cycle and allow for slopes to be calculated at SOD extremes. Selecting an appropriate measurement period requires some trial and error, and we recommend testing several measurement period lengths to determine the optimal settings. SOD incubation measurements may also be optimized by changing the depth to which the chambers are pushed into the sediment, and therefore the volume of the overlying water in the chamber; for example, in highly active sediments a greater incubated water volume would be more appropriate to prevent sharp drops in DO during the incubations.

The flush duration is set by changing the amount of time each chamber flush pump is turned on at the beginning of each measurement period. There is little risk of over-flushing, however, under flushing may result in incomplete exchange of the chamber overlying water. This would be noticeable as several successive sawtooth peaks not matching with the ambient DO at the start of each measurement period. The pumps used in our setup were set to pump $\sim 100 \text{ mL s}^{-1}$ and the overlying volume of the chambers was $\sim 1 \text{ L}$, so pumps were left on for 20 s each, or twice the amount of time needed to flush the chambers assuming perfect replacement of water. Our test deployment took place in sandy sediments regularly exposed to high wave action, so disturbance of sediment within the chamber from flushing was of low concern. However, in finer-grained, muddier, consolidated sediments the pump rate should be slowed to prevent chamber flushing from eroding the sediment. This could be done by directly restricting the intake of water for each chamber flush pump, that is, by covering with screen mesh or attaching an adapter with a smaller diameter opening, or by branching the tubing from a single pump to multiple chambers, therefore, decreasing flow rate to each chamber. Note that with a decreased flow

rate the flush time will have to be increased to ensure sufficient chamber flushing.

The mixing conditions can be set by changing the amount of time the mixing pump is turned on vs. off during each loop, and the amount of mixing time necessary may vary depending on the pump and the mixing apparatus in the chamber. Our mixing pump had a high flow rate and power draw, so we turned them on intermittently to avoid over-mixing the chambers in addition to conserving battery power. In setups using mixing pumps with lower-flow rates and power draws, we recommend increasing the amount of time spent mixing as much as possible. We would also recommend if at all possible constructing the mixing apparatus to be easily adjustable such that mixing regimes inside the chambers may be matched to a wide variety of environments. This may be done by using a separate mixing pump with an adjustable flow rate for each of the chambers rather than a single mixing pump plumbed to all the chambers in series.

If the system is to be deployed from a boat in deeper water, we recommend affixing the central housing and five 5 gal screw-lid buckets to a fiberglass platform and placing the chambers in the buckets for deployment. The entire platform may then be lowered into the water, and divers descend to deploy the chambers and turn the system on. For retrieval, the divers should extract each core with the enclosed sediment intact and seal the bottom with a rubber plug or cap, return the cores to the buckets on the platform, and then the platform raised back onto the boat.

REFERENCES

Aller, R. C. 1978. The effects of animal-sediment interactions on geochemical processes near the sediment-water interface, p. 157–172. In M. L. Wiley [ed.], *Estuarine interactions*. Academic Press. doi:[10.1016/B978-0-12-751850-3.50017-0](https://doi.org/10.1016/B978-0-12-751850-3.50017-0)

Arega, F., and J. H. Lee. 2005. Diffusional mass transfer at sediment–water interface of cylindrical sediment oxygen demand chamber. *J. Environ. Eng.* **131**: 755–766. doi:[10.1061/\(ASCE\)0733-9372\(2005\)131:5\(755\)](https://doi.org/10.1061/(ASCE)0733-9372(2005)131:5(755)

Attard, K. M., H. Stahl, N. A. Kamenos, G. Turner, H. L. Burdett, and R. N. Glud. 2015. Benthic oxygen exchange in a live coralline algal bed and an adjacent sandy habitat: An eddy covariance study. *Mar. Ecol. Prog. Ser.* **535**: 99–115. doi:[10.3354/meps11413](https://doi.org/10.3354/meps11413)

Berg, P., and M. Huettel. 2008. Monitoring the seafloor using the noninvasive eddy correlation technique. *Oceanography* **21**: 164–167. doi:[10.5670/oceanog.2008.13](https://doi.org/10.5670/oceanog.2008.13)

Berg, P., H. Roy, F. Janssen, V. Meyer, B. B. Jorgensen, M. Huettel, and D. de Beer. 2003. Oxygen uptake by aquatic sediments measured with a novel non-invasive eddy-correlation technique. *Mar. Ecol. Prog. Ser.* **261**: 75–83. doi:[10.3354/meps261075](https://doi.org/10.3354/meps261075)

Berg, P., H. Røy, and P. L. Wiberg. 2007. Eddy correlation flux measurements: The sediment surface area that contributes to the flux. *Limnol. Oceanogr.* **52**: 1672–1684. doi:[10.1002/lim3.10571](https://doi.org/10.1002/lim3.10571)

Berg, P., R. N. Glud, A. Hume, H. Stahl, K. Oguri, V. Meyer, and H. Kitazato. 2009. Eddy correlation measurements of oxygen uptake in deep ocean sediments. *Limnol. Oceanogr.: Methods* **7**: 576–584. doi:[10.4319/lom.2009.7.576](https://doi.org/10.4319/lom.2009.7.576)

Berg, P., and others. 2013. Eddy correlation measurements of oxygen fluxes in permeable sediments exposed to varying current flow and light. *Limnol. Oceanogr.* **58**: 1329–1343. doi:[10.4319/lo.2013.58.4.1329](https://doi.org/10.4319/lo.2013.58.4.1329)

Berg, P., M. Huettel, R. N. Glud, C. E. Reimers, and K. M. Attard. 2022. Aquatic eddy covariance: The method and its contributions to defining oxygen and carbon fluxes in marine environments. *Ann. Rev. Mar. Sci.* **14**: 431–455. doi:[10.1146/annurev-marine-042121-012329](https://doi.org/10.1146/annurev-marine-042121-012329)

Burdige, D. J. 2006. *Geochemistry of marine sediments*. Princeton Univ. Press.

Camillini, N., K. Attard, B. Eyre, and R. Glud. 2021. Resolving community metabolism of eelgrass *Zostera marina* meadows by benthic flume-chambers and eddy covariance in dynamic coastal environments. *Mar. Ecol. Prog. Ser.* **661**: 97–114. doi:[10.3354/meps13616](https://doi.org/10.3354/meps13616)

Du, J., K. Park, J. Shen, B. Dzwonkowski, X. Yu, and B. I. Yoon. 2018. Role of baroclinic processes on flushing characteristics in a highly stratified estuarine system, Mobile Bay, Alabama. *J. Geophys. Res.: Oceans* **123**: 4518–4537. doi:[10.1029/2018JC013855](https://doi.org/10.1029/2018JC013855)

Glud, R., S. Forster, and M. Huettel. 1996. Influence of radial pressure gradients on solute exchange in stirred benthic chambers. *Mar. Ecol. Prog. Ser.* **141**: 303–311. doi:[10.3354/meps141303](https://doi.org/10.3354/meps141303)

Johengen, T., and others. 2016. Performance verification statement for onset's HOBO U26 dissolved oxygen sensors. 013. 013. Alliance for Coastal Technologies. doi:[10.25607/OPB-296](https://doi.org/10.25607/OPB-296)

Jørgensen, B. B., F. Wenzhöfer, M. Egger, and R. N. Glud. 2022. Sediment oxygen consumption: Role in the global marine carbon cycle. *Earth Sci. Rev.* **228**: 103987. doi:[10.1016/j.earscirev.2022.103987](https://doi.org/10.1016/j.earscirev.2022.103987)

Juska, I., and P. Berg. 2022. Variation in seagrass meadow respiration measured by aquatic eddy covariance. *Limnol. Oceanogr.: Lett.* **7**: 410–418. doi:[10.1002/lol2.10276](https://doi.org/10.1002/lol2.10276)

Kononets, M., and others. 2021. In situ incubations with the Gothenburg benthic chamber landers: Applications and quality control. *J. Mar. Syst.* **214**: 103475. doi:[10.1016/j.jmarsys.2020.103475](https://doi.org/10.1016/j.jmarsys.2020.103475)

Middelburg, J. J., and L. A. Levin. 2009. Coastal hypoxia and sediment biogeochemistry. *Biogeosciences* **6**: 1273–1293. doi:[10.5194/bg-6-1273-2009](https://doi.org/10.5194/bg-6-1273-2009)

Tengberg, A., and others. 1995. Benthic chamber and profiling landers in oceanography—A review of design, technical solutions and functioning. *Prog. Oceanogr.* **35**: 253–294. doi:[10.1016/0079-6611\(95\)00009-6](https://doi.org/10.1016/0079-6611(95)00009-6)

Tengberg, A., H. Stahl, G. Gust, V. Müller, U. Arning, H. Andersson, and P. O. J. Hall. 2004. Intercalibration of benthic flux chambers I. Accuracy of flux measurements and influence of chamber hydrodynamics. *Prog. Oceanogr.* **60**: 1–28. doi:[10.1016/j.pocean.2003.12.001](https://doi.org/10.1016/j.pocean.2003.12.001)

Volkenborn, N., L. Polerecky, D. S. Wethey, and S. A. Woodin. 2010. Oscillatory porewater biaudvection in marine sediments induced by hydraulic activities of *Arenicola marina*. *Limnol. Oceanogr.* **55**: 1231–1247. doi:[10.4319/lo.2010.55.3.1231](https://doi.org/10.4319/lo.2010.55.3.1231)

Webb, B. M., and C. Marr. 2016. Spatial variability of hydrodynamic timescales in a broad and shallow estuary: Mobile Bay, Alabama. *J. Coast. Res.* **32**: 1374–1388. doi:[10.2112/JCOASTRES-D-15-00181.1](https://doi.org/10.2112/JCOASTRES-D-15-00181.1)

Wenner, E., D. Sanger, M. Arendt, A. F. Holland, and Y. Chen. 2004. Variability in dissolved oxygen and other water-quality variables within the national estuarine research reserve system. *J. Coast. Res.* **100**: 17–38. doi:[10.2112/SI45-017.1](https://doi.org/10.2112/SI45-017.1)

Wenzhöfer, F., and R. N. Glud. 2004. Small-scale spatial and temporal variability in coastal benthic O₂ dynamics: Effects of fauna activity. *Limnol. Oceanogr.* **49**: 1471–1481. doi:[10.4319/lo.2004.49.5.1471](https://doi.org/10.4319/lo.2004.49.5.1471)

Zorn, M. E., S. V. Lalonde, M. K. Gingras, S. G. Pemberton, and K. O. Konhauser. 2006. Microscale oxygen distribution in various invertebrate burrow walls. *Geobiology* **4**: 137–145. doi:[10.1111/j.1472-4669.2006.00074.x](https://doi.org/10.1111/j.1472-4669.2006.00074.x)

Acknowledgments

Thank you to Will Ballentine, Chesna Cox, Jenna Moore, and Madeline Frey for assisting with chamber test deployments, Brian Dzwonkowski for providing the field opportunity to seal-test the chamber housing, John Lehrter, Behzad Mortazavi, and Sarah Berke for helpful discussions and advice, and two reviewers for valuable feedback. This work was funded by NSF OCE CAREER Grant 1844910 and ONR Award N00014-18-1-2806 to KMD, the University of South Alabama Center for Environmental Resiliency, and the Southern Association of Marine Laboratories Student Support Program.

Conflict of Interest

None declared.

Submitted 24 January 2023

Revised 14 July 2023

Accepted 02 August 2023

Associate editor: Paul F. Kemp